X-ray backscatter sensing of defects in carbon fibre composite materials

Daniel O'Flynn[a], Chiaki Crews*[a], Nicholas Fox[b], Brian P. Allen[c], Mark Sammons[b], Robert D. Speller[a]
[a]Dept. of Medical Physics and Biomedical Engineering, University College London, UK; [b]Axi-Tek Ltd., Loughborough, UK; [c]QinetiQ Ltd., Farnborough, UK

ABSTRACT

X-ray backscatter (XBS) provides a novel approach to the field of non-destructive evaluation (NDE) in the aerospace industry. XBS is conducted by collecting the radiation which is scattered from a sample illuminated by a well-defined X-ray beam, and the technique enables objects to be scanned at a sub-surface level using single-sided access, and without the requirement for coupling with the sample. Single-sided access is of particular importance when the objects of interest are very large, such as aircraft components. Carbon fibre composite materials are being increasingly used as a structural material in aircraft, and there is an increasing demand for techniques which are sensitive to the delaminations which occur in these composites as a result of both large impacts and barely visible impact damage (BVID). The XBS signal is greatly enhanced for plastics and lightweight materials, making it an ideal candidate for probing sub-surface damage and defects in carbon fibre composites. Here we present both computer modelling and experimental data which demonstrate the capability of the XBS technique for identifying hidden defects in carbon fibre.

Keywords: X-ray backscatter, BVID, NDE, carbon fibre composites

1. INTRODUCTION

1.1 X-ray backscatter

X-ray backscatter (XBS) occurs as a result of Compton scattering, an incoherent, inelastic process where the energy of the scattered photon is different to that of the incident photon, as shown in Figure 1. This difference in energy depends on the angle of scatter (θ) and the incident X-ray wavelength. Generally, for X-ray energies of up to 100keV, Compton scatter occurs in all directions. Thus, single-sided interrogation of a material is possible by directing an X-ray beam at an object, and detecting backscattered X-rays – those emerging at an angle $270° > \theta > 90°$ – across an area of interest to construct an image[1].

The probability of Compton scatter depends on the electron density of the material, which in turn is dependent on Z_{eff} and physical density. However, because absorption effects are dominant in high Z_{eff} materials, XBS is enhanced for lower Z_{eff} materials such as carbon fibre composites.

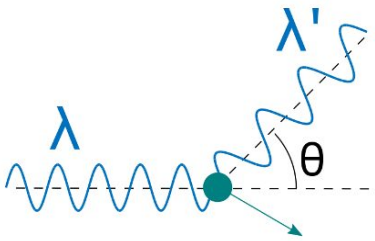

Figure 1. Diagram depicting an incident X-ray of wavelength λ being inelastically scattered by an electron, resulting in an X-ray of wavelength λ' and recoil electron

This technique has been applied in the fields of security (e.g. screening passengers at airports[2], as well as trucks and cars[3]), medicine (e.g. assessing bone density[4]), and aerospace[5], plus has potential applications in many others such as oil and gas drilling[6] and food inspection[7].

*E-mail: chiaki.crews.10@ucl.ac.uk

Advanced Photon Counting Techniques XI, edited by Mark A. Itzler, Joe C. Campbell, Proc. of SPIE
Vol. 10212, 102120R · © 2017 SPIE · CCC code: 0277-786X/17/$18 · doi: 10.1117/12.2262581

1.2 Carbon fibre composites and aircraft NDE

Carbon fibre composite materials consist of layers of woven carbon fibres that are embedded in a resin matrix. The specific method of weaving and layering as well as the type of resin used can be varied and depends on the intended application[8]. Due to their very high strength-to-weight ratio, these materials have been increasingly incorporated into aircraft, such as the Airbus A380 and Boeing 787 Dreamliner[9].

However, the use of such materials has introduced novel challenges in the area of aircraft NDE, as the defects caused by impacts and fatigue on carbon fibre composites differ to those in more traditional metallic structures. Notably, delaminations – when the layers within the composite separate – are one of the most common defects that can occur[10]. NDE methods that are currently used include eddy current, ultrasonics, electrochemical methods, thermography, dye penetrant, tap testing, and radiographic inspection (both transmission and backscatter)[9,11,12], but not all are applicable to composite materials.

Ultrasonics is currently the standard test modality, but has disadvantages of signal interpretation and the requirement of acoustic coupling agents[13]. XBS has potential in this area as it does not require sample preparation, has an enhanced signal in lightweight materials, and only requires single-sided access[11] – making it practical for use on large structures such as aircraft.

2. METHODOLOGY

2.1 Monte Carlo model setup

FLUKA software (v2011.2c.4) was used to create models of XBS experimental setups and run Monte Carlo simulations in order to assess the ability to detect subsurface defects of interest in carbon composites. The input parameters that were required for these models are depicted in Figure 2.

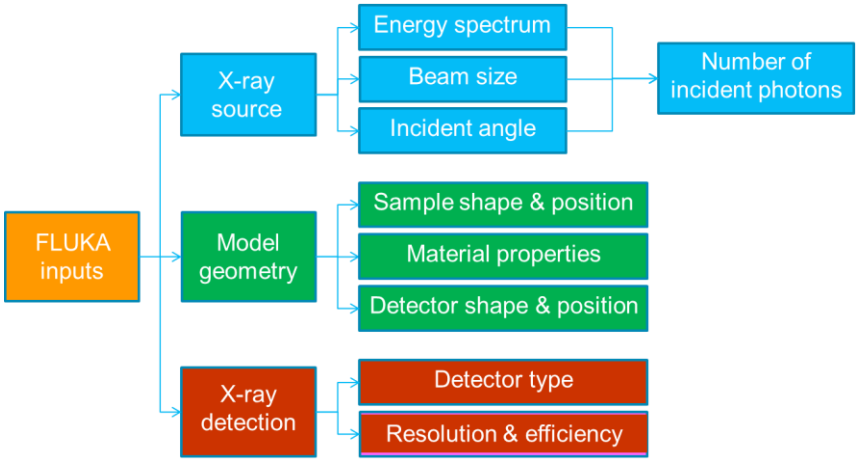

Figure 2. Diagram of input parameters to models

The spectra for a tungsten X-ray source operated at 50kVp and 80kVp were generated using SpekCalc software[14]. A 1mm-diameter pencil beam was used in all simulations.

The following molecular weightings were inputted to simulate the carbon fibre composite samples: 67% carbon, 21% hydrogen, 4% nitrogen, and 8% oxygen; they were presumed to have a density of 1.7gcm^{-3} [15]. Defects were introduced as voids of air within samples, and various shapes were tested.

The 'detector' was a cuboid where the number and energy of any photons that passed through the face nearest the sample were measured. FLUKA had the option to modify detector efficiency, outputting the energy deposited in the detector per photon; this measure or a simple sum of counts were used for our analyses. The energy spectra of incident and transmitted X-rays were also recorded.

2.2 Monte Carlo simulations

An X-ray beam (set to 50kVp) was scanned across carbon fibre composite samples, with incident X-rays perpendicular to the sample surface. In the first scenario, a 3mm-diameter cylindrical void was introduced into the sample (Figure 3A); a crack perpendicular to the sample surface (Figure 3B) and an in-plane defect (Figure 3C) were also simulated. All voids were positioned at 3mm depth into a 7mm-thick carbon fibre composite sample.

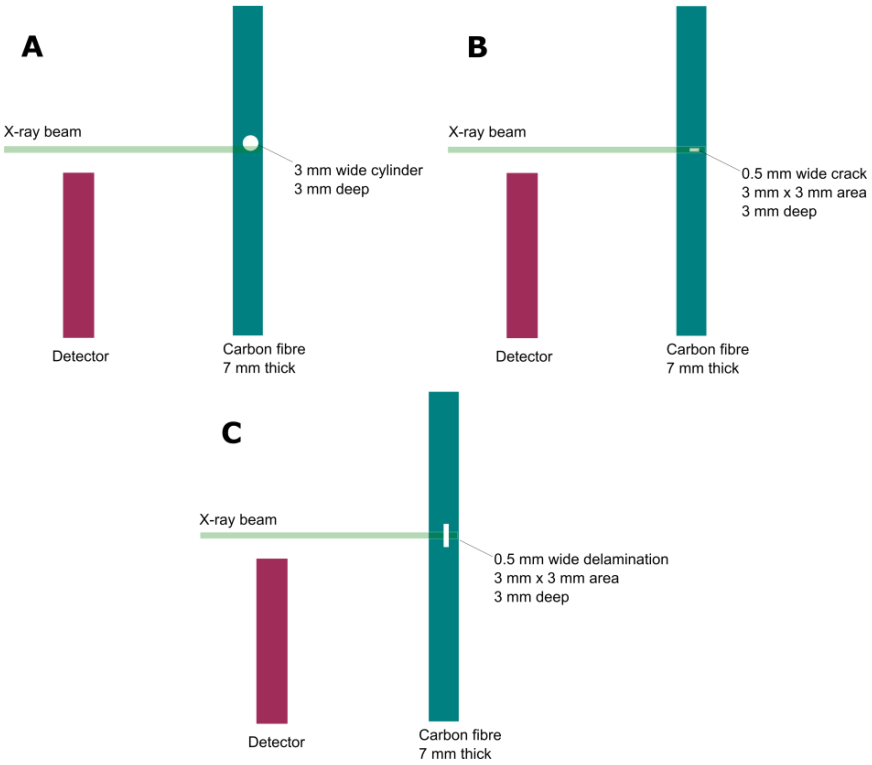

Figure 3. Diagram showing Monte Carlo simulation setups: (A) with a cylindrical void; (B) with a crack; (C) with an in-plane 'delamination'

In-plane defects are of greater interest due to their closer similarity to a delamination. A layered delamination was modelled by a series of ten in-plane 100µm x 3mm x 3mm air gaps, separated by 125µm of composite material (Figure 4). This feature was positioned at the back (relative to incident X-rays) of the sample panel, as this is where delaminations tend to occur when there is an impact on the outer surface of fuselage. The total sample thickness was also varied: 3, 5, 8, 10, 15, 20, 30, 40, and 50mm-thick samples were modelled. An incident X-ray beam (80kVp) at an acute incident angle was used, as earlier simulations suggested that this would improve the XBS signal.

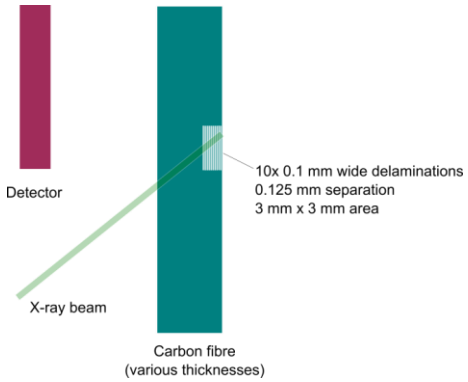

Figure 4. Monte Carlo model setup for layered delamination simulations

2.3 Experimental setup

An X-ray source (Source-Ray Inc. SB-80-1K) with a 1mm pinhole collimator was mounted on a rotation stage such that the incident X-ray angle could be modified. Vertical and horizontal translation stages were used for remote sample positioning. All motion stages were controlled via a Newport XPS-Q8 controller. A compact, mains-operated energy-resolving CdTe detector (Amptek X-123) with a 5mm^2 active area and 0.1mm Be window was used to collect the backscattered X-rays.

A graphical user interface (GUI) was created in Matlab (MathWorks R2015a), allowing the user to input start and end positions, step sizes (min. 10µm), and scan time at each step, such that the data acquisition was synchronised with the movement of the sample stages. The outputted data files contained information on the recorded spectra at specified stage positions (horizontal and vertical) and an additional file with the summed total counts from the spectra at each point. The GUI also displayed a plot of the XBS spectrum collected at the last point, and a pixellated colour map of summed counts for all positions scanned, both of which updated automatically as the scan progressed.

2.4 Carbon fibre panel scans

A 3.5mm-thick carbon fibre composite panel that had been impacted in five positions using a laboratory hemispherical impactor was scanned. The central impact had caused the most damage, and a second impact had also resulted in a visible distortion on the back surface of the panel (circled in Figure 5). A CT scan of the panel clearly showed the delaminations that had occurred as a result of both these impacts; no defects caused by the other three were evident (data not shown).

A pencil X-ray beam (80kV, 1mA) was scanned across the front face of the panel (i.e. impacted side, left image in Figure 5) in the two regions with known delaminations. A step size of 1mm and acquisition time of 15s/step was used. The summed counts from the collected XBS spectra at each point were used to create an image of the two defects.

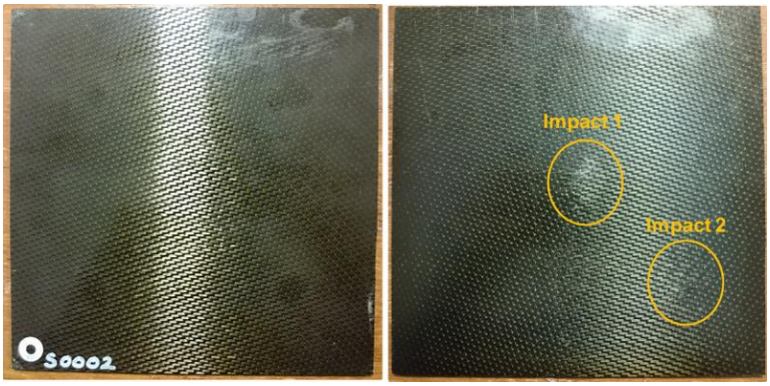

Figure 5. Photographs of the scanned carbon fibre composite panel; (left) front – impacted side and (right) back (two delaminations visible)

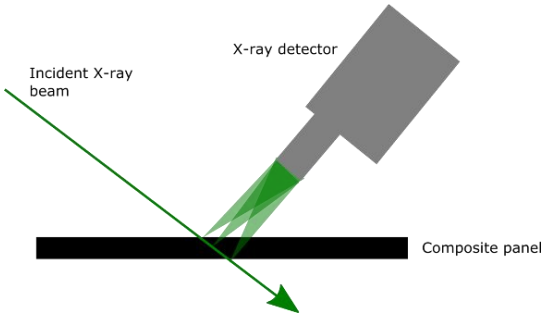

Figure 6. Experimental setup

3. RESULTS AND DISCUSSION

3.1 Monte Carlo simulations

The result of the simulation described in Figure 3A is shown in Figure 7. In general, a defect was detected where the XBS signal – normally from scattered X-rays at all depths within a sample – dropped off due to there being less material present. In addition to this, there was a noticeable rise in scatter collected when the X-rays were incident on the edge of the defect that was furthest from the detector. This can be explained by the fact that the scattered X-rays at this point are attenuated by less material before reaching the detector compared to those scattered from further up the panel (as illustrated by the diagrams within Figure 7).

Figure 8 shows the result of scanning the 0.5mm crack defect (Figure 3B), and demonstrates how the position of the detector affected which side the rise in counts was observed.

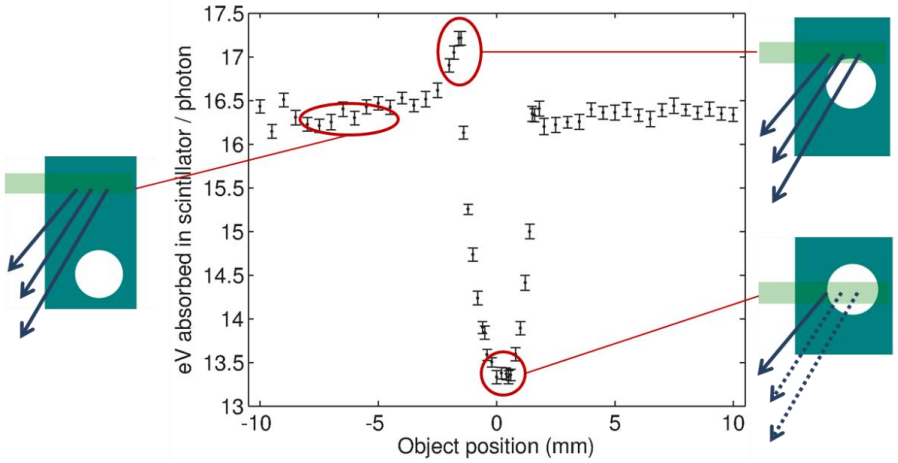

Figure 7. Result of simulation of cylindrical void at 3mm depth; diagrams show example of path taken by backscattered photons prior to reaching detector

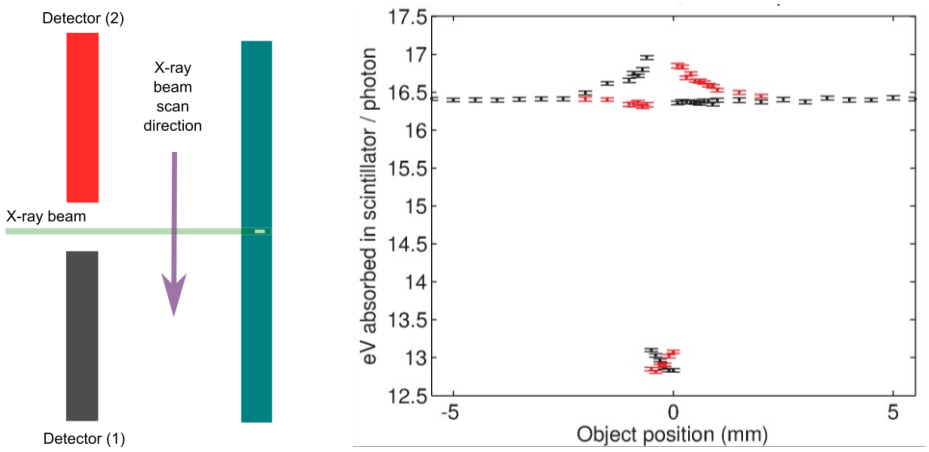

Figure 8. Result of simulation of 0.5mm-wide crack at 3mm depth with detector in position 1 (black) and 2 (red)

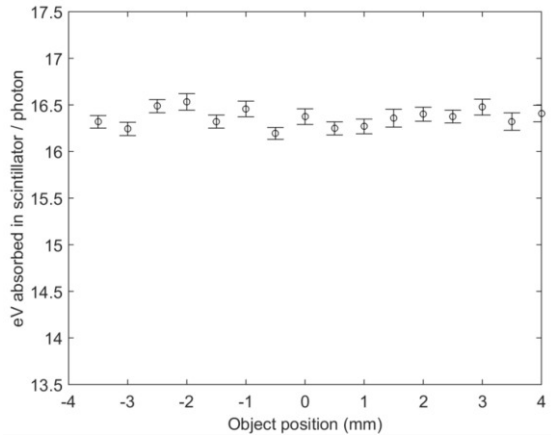

Figure 9. Result of simulation of 0.5mm in-plane 'delamination' at 3mm depth

However, the in-plane defect (Figure 3C) resulted in no obvious XBS signal contrast at the defect site, as shown in Figure 9. It was found that X-rays incident at an acute angle to the sample surface were more effective at detecting such defects, as the voids constituted a larger portion of the scatter volume in this geometry.

The XBS results from layered delaminations simulated with an acute incident X-ray angle are presented in Figure 10. The plots for each sample thickness show the normalised summed counts from the XBS spectra at each position. Blue circles were calculated from the full spectra, whereas the pink dots only used counts from the energy range shown, chosen to give the highest signal-to-noise-ratio after iteratively changing the lower energy threshold.

The delamination signal was apparent even up to a 50mm-thick sample, although the SNR was significantly degraded beyond 30mm of thickness (i.e. with the delamination appearing from 27.75mm depth).

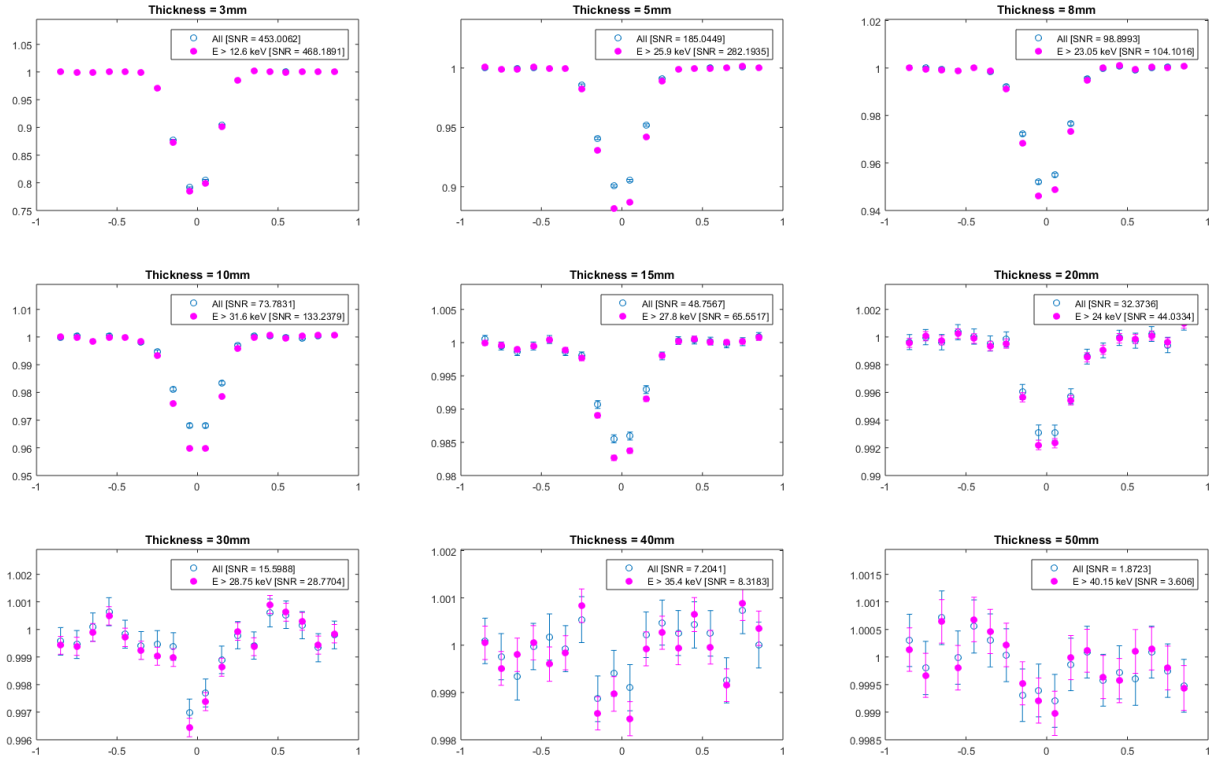

Figure 10. Plots of normalised counts vs. position in sample (in cm) for layered delaminations simulated at rear of carbon fibre composite panel of various thicknesses

3.2 Experimental results

The data acquired with the experimental XBS system are presented in Figure 11. The delaminations were clearly revealed by the contrast in counts compared to the surrounding undamaged material. The line scans show slices through the strongest drop in XBS signal; this confirmed that there was a rise in counts on one side of the defect, as simulations had predicted. This explains the brighter regions in the images, corresponding to the defect edge that was furthest from the detector during the scan.

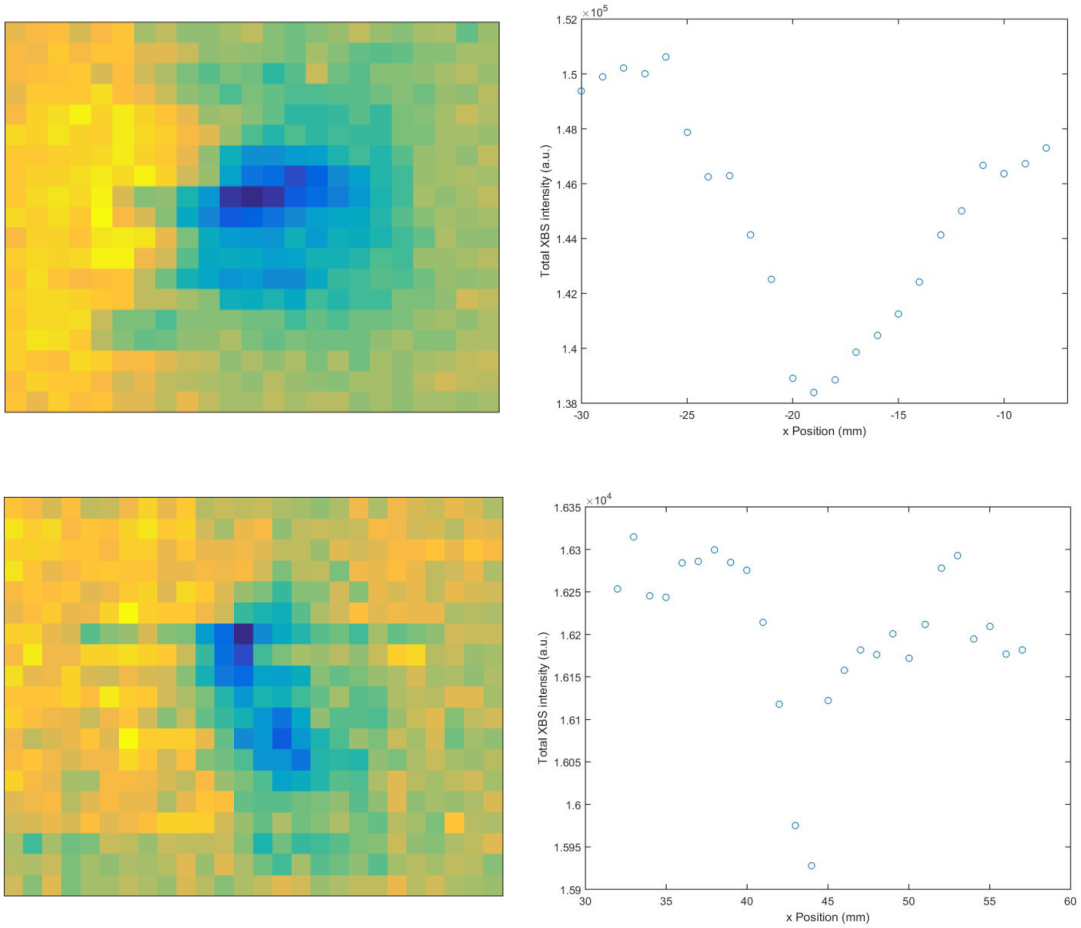

Figure 11. XBS images and line scans through delamination caused by 'Impact 1' (top) and 'Impact 2' (bottom)

4. CONCLUSIONS

The results of simulations successfully predicted the way in which delaminations in carbon fibre composites would appear under experimental conditions. The effect of the increase in XBS signal on one side of a defect needs to be investigated further; it may be advantageous to use this signal to alert a user to the presence of a defect in addition to the fall in counts that follows.

Although the sample used for this initial experiment had not been subjected to surface treatments such as lighting strike protection (copper mesh) and paint, the potential of XBS for aircraft NDE is apparent and further work is under progress. There is much scope for optimising the defect detection capability of the experimental system by modifying various parameters such as the X-ray flux, beam collimation size, incidence angle, scanning step size, counting time, and detector characteristics.

Note: The authors would like to acknowledge Dr Neil O'Brien at the University of Southampton, UK, for acquiring the CT scans on the impacted test sample.

REFERENCES

[1] Towe, B. C., Jacobs, A. M., "X-Ray Backscatter Imaging," IEEE Trans. Biomed. Eng. **BME-28**(9), 646–654 (1981).
[2] Kaufman, L., Carlson, J. W., "An evaluation of airport x-ray backscatter units based on image characteristics," J. Transp. Secur. **4**(1), 73–94 (2011).
[3] Callerame, J., "X-ray backscatter imaging: Photography through barriers," Powder Diffr. **21**(2), 132–135, Cambridge University Press (2006).
[4] Garnett, E. S., Kennett, T. J., Kenyon, D. B., Webber, C. E., "A Photon Scattering Technique for the Measurement of Absolute Bone Density in Man," Radiology **106**(1), 209–212, The Radiological Society of North America (1973).
[5] Kolkoori, S., Wrobel, N., Zscherpel, U., Ewert, U., "A new X-ray backscatter imaging technique for non-destructive testing of aerospace materials," NDT E Int. 70, 41-52 (2015).
[6] Spannuth, M., Esmaeili, M., Gunn, S., Ponce-Marquez, D. M., Torsteinsen, H.., Voll, A., "X-ray Backscatter Imaging in an Oil Well," SPE Annu. Tech. Conf. Exhib., Society of Petroleum Engineers (2014).
[7] McFarlane, N. J. B., Bull, C. R., Tillett, R. D., Speller, R. D., Royle, G. J., "Time Constraints on Glass Detection in Food Materials using Compton Scattered X-rays," J. Agric. Eng. Res. **79**(4), 407–418 (2001).
[8] Soutis, C., "Fibre reinforced composites in aircraft construction," Prog. Aerosp. Sci. **41**(2), 143–151 (2005).
[9] Diamanti, K., Soutis, C., "Structural health monitoring techniques for aircraft composite structures," Prog. Aerosp. Sci. **46**(8), 342–352, Elsevier (2010).
[10] Cheng, L., Tian, G. Y., "Comparison of nondestructive testing methods on detection of delaminations in composites," J. Sensors **2012**, 1-7 (2012).
[11] Dunn, W. L., Yacout, A. M., "Corrosion detection in aircraft by X-ray backscatter methods," Appl. Radiat. Isot. **53**(4–5), 625–632 (2000).
[12] Kamsu-Foguem, B., "Knowledge-based support in Non-Destructive Testing for health monitoring of aircraft structures," Adv. Eng. Informatics **26**(4), 859–869 (2012).
[13] Shull, P. J., [Nondestructive evaluation: theory, techniques, and applications], CRC Press, Taylor & Francis Group, Boca Raton, (2002).
[14] Poludniowski, G., Landry, G., DeBlois, F., Evans, P. M., Verhaegen, F., "*SpekCalc* : a program to calculate photon spectra from tungsten anode x-ray tubes," Phys. Med. Biol. **54**(19), N433–N438, IOP Publishing (2009).
[15] Gupta, V. B., Kothari, V. K., [Manufactured fibre technology], Chapman & Hall (1997).